Archaeological Prospection
Archaeol. Prospect. **20**, 163–174 (2013)
Published online 6 May 2013 in Wiley Online Library
(wileyonlinelibrary.com) DOI: 10.1002/arp.1450

Microgravity and Ground-penetrating Radar Investigations of Subsurface Features at the St Catherine's Monastery, Slovakia

JAROSLAVA PANISOVA[1]*, MAREK FRAŠTIA[2], TINA WUNDERLICH[3], ROMAN PAŠTEKA[4] AND DAVID KUŠNIRÁK[4]

[1] *Geophysical Institute, Slovak Academy of Sciences, Dúbravská cesta 9, 845 28 Bratislava, Slovakia*
[2] *Department of Surveying, Faculty of Civil Engineering, Slovak University of Technology, Radlinského 11, 813 68 Bratislava, Slovakia*
[3] *Institute of Geosciences, Department of Geophysics, Christian-Albrechts-University, Otto-Hahn-Platz 1, 24118 Kiel, Germany*
[4] *Department of Applied and Environmental Geophysics, Faculty of Natural Sciences, Comenius University, Mlynská dolina, 842 15 Bratislava, Slovakia*

ABSTRACT The ruins of the St Catherine's monastery complex, the largest sacral ruins in Slovakia, are an important example of Slovak cultural heritage. The Franciscan monastery was a famous site of religious significance due to the legends describing the apparitions of St Catherine. The preservation project of the monastery remains started in 1994. As a part of this project, complex historical, archaeological, anthropological and geophysical research has been conducted at the site since 1997. Microgravity and ground-penetrating radar (GPR) surveys were carried out in the nave of the former church in order to reveal the position of three aristocratic crypts that served as burial places for the members or higher society in the seventeenth and eighteenth centuries. In the microgravity data processing, a novel method for the calculation of the building correction was employed, where the gravitational effect of the church is calculated using a polyhedral model of the building created from photographs with a special photogrammetric software. Several gravity anomalies were found in the residual Bouguer anomaly map. Semi-automated interpretation techniques including the Euler deconvolution and harmonic inversion have been used to investigate the depth and size of anomalous sources. Results from 36 GPR profiles obtained by a 400 MHz antenna were visualized in the form of horizontal time-slices and vertical time-sections. These images indicate anomalous reflections suggesting potential archaeological targets. Integrated interpretation of results from both geophysical methods has confirmed the presence of a known aristocratic crypt excavated in 2001, as well as two other crypts predicted from historical archives. The combination of microgravity and GPR surveys has proved to be a very effective and non-destructive tool for archaeological research. Copyright © 2013 John Wiley & Sons, Ltd.

Key words: Microgravity; ground-penetrating radar; digital photogrammetry; crypt detection; cultural heritage; Slovakia

Introduction

The ruins of St Catherine's monastery are located on a rocky hill in the woods of the Little Carpathians in western Slovakia, 20 km northwest from Trnava (inset in Figure 1). The geology of the site consists of Middle Triassic carbonates (light-coloured massive limestones of the Nedzov nappe) and Quaternary sediments. The Franciscan monastery was founded in 1618 in an area where the Gothic chapel from the fifteenth century dedicated to St Catherine of Alexandria was situated. The original monastery church was rebuilt in 1646 as a larger Early Baroque object with dimensions of 52 m and 13.5 m and with a tower 30 m high. The presbytery of the church was built on stone foundations of the former Gothic chapel. The monastery

*Correspondence to: J. Panisova, Geophysical Institute, Slovak Academy of Sciences, Dúbravská cesta 9, 845 28 Bratislava, Slovakia. E-mail: geofjapa@savba.sk

Received 10 October 2012
Accepted 7 April 2013

Figure 1. Aerial photograph of the St Catherine's monastery ruins (Herceg, 2009). The inset shows a map of the location of the site. (Herceg, personal communication, 2012, photo used with the permission of the author). This figure is available in colour online at wileyonlinelibrary.com/journal/arp

complex was invaded several times by the Turks and emperor's army in the seventeenth century. The St Catherine's monastery was abolished by the order of the Emperor Joseph the Second in 1786 (Herceg, 2009). Nowadays, only the ruins of the church and the remains of the southern part of the monastery walls are preserved (Figure 1).

From historical sources (mainly the canonical visitations in the seventeenth and eighteenth centuries archived in the Roman Catholic Manse in Dechtice) we know the description of the church, monastery and its surroundings. Important is the mention of the presence of crypts in the nave of the church, which belonged to rich aristocratic families, such as Erdődy, Apponyi and Labsánszky. It is also stated that the crypt entrances did not conform to the royal regulation and due to the fact that the church was build on hard rock, there was only one entry into each crypt (Matulová, 2003).

The present restoration of the ruins started in 1994 (Herceg, 2009). The St Catherine's monastery preservation project is organized by a local civil association in cooperation with the Association of the Christian Youth Communities in Slovakia. In the framework of this project, complex historical, archaeological, anthropological and geophysical research has been conducted at the site since 1997. In the framework of the realized archaeological survey several parts of the monastery walls have been exposed, as well as locating the foundations of the former Gothic chapel in the present presbytery and one small external chapel in the northern part of the monastery complex. The first geophysical survey was carried out in the nave of the former St Catherine's church in 1999. On the basis of the results from microgravity and resistivity imaging, four anomalous areas indicating the presence of cavities were delineated. Consequently, a medieval partially filled crypt was discovered in the area of the largest gravity low (Pašteka and Zahorec, 2000).

Archaeological excavation of this crypt (Figure 2) was undertaken in 2001 (Urminský, 2002). Although the crypt was filled by the debris from the destroyed vaulted ceiling and was robbed by grave robbers in the nineteenth century, interesting anthropological findings were uncovered. Skeletal remains of at least 26 individuals mixed with the soil filling were found in non-anatomical positions during the excavation. The results of the trace element analysis indicated that the examined individuals were most likely members of a higher society; they could belong to an aristocratic family (Bodoriková *et al.*, 2010). The crypt, divided by a cross-wall at one-third of its length, has a rectangular shape with dimensions of $5 \times 1.9 \times$ approximately 2 m (Figure 2). The entrance stairs were cut into the rocky bedrock that crops out to the surface just about the centre line of the nave. After excavation, the crypt was covered by concrete joists embedded on isolated footings, which are easily removable. This frame is covered by hydro-isolation and geotextile and backfilled to the level of the previous terrain (Herceg, 2009).

DOI: 10.1002/arp

Figure 2. East view on the crypt excavated in 2001 (Herceg, 2009). (Herceg, personal communication, 2012, photo used with the permission of the author). This figure is available in colour online at wileyonlinelibrary.com/journal/arp

Figure 3. Three-dimensional textured model of the church, obtained by photo-based scanning. This figure is available in colour online at wileyonlinelibrary.com/journal/arp

St Catherine's monastery ruins were also documented using photogrammetric methods. For example, detailed ground plans, digital orthophoto maps of the walls and precise three-dimensional models of the ruins were created. Figure 3 shows the three-dimensional textured model of the church obtained by photo-based scanning as an example of photogrammetric recording of the monastery remains. In addition to photogrammetric recordings, this paper describes the results of the ground-penetrating radar (GPR) and microgravity surveys carried out in the nave of the church in 2011 in the framework of a field course for students of geophysics from German and Slovak universities. The main objectives for these surveys were (i) to map the shallow parts of the subsurface using geophysical methods and (ii) to identify archaeological anomalies, i.e. potential areas for further archaeological research.

Rectangular prisms or vertical prisms with polygonal cross-sections are commonly used to approximate the buildings in microgravity surveys if the gravity data needs to be corrected for these gravitational effects (e.g. Blížkovský, 1979; Pašteka and Zahorec, 2000; Debeglia and Dupont, 2002; Padín *et al*., 2012). In the paper a novel method for the calculation of building effects in microgravity data processing was used, where geodetic and photogrammetric measurements are combined to obtain a three-dimensional model of the historical monument. This interdisciplinary approach allows highly detailed and precise virtual models of measured objects to be created, thus increasing the accuracy of the calculated building correction (Panisova *et al*., 2012).

Photogrammetric processing

Photogrammetry is the measurement technique that reconstructs the position and shape of physical objects through the process of recording, measuring and interpreting photographic images. A range of techniques and photographic equipment is available to generate three-dimensional digital models of archaeological monuments. The fundamental principle consists in the mathematical model of central projection by compensating systematic errors during bundle adjustment, which gives the adjusted parameters of internal and external camera orientation and the spatial

DOI: 10.1002/arp

coordinates of the observed points (Luhmann *et al*., 2006). The methods of projective photogrammetry, convergent photogrammetry and optical scanning are widely applied in the preservation of architectural heritage and archaeological investigations (Luhmann *et al*., 2006). The capability of close-range photogrammetry to improve microgravity data processing is introduced in Panisova *et al*. (2012), where a new method for the calculation of the building corrections based on photogrammetric reconstruction was used.

The convergent multistation photogrammetric method has been applied for the digital spatial reconstruction of the church. The images were taken with digital cameras Olympus C-8080 (lenses Olympus $f = 7.1–35.6$ mm) and Nikon D-200 (lenses Nikkor $f = 20$ mm). Both cameras were calibrated in the test and calibration field (Fraštia, 2005) before image acquisition.

The photogrammetric processing of the project was carried out using the PhotoModeler 6 software (www.photomodeler.com). Characteristic points of the object have been measured on digital images manually, within an accuracy of 1–2 pixels depending on point identification. Subsequently, spatial coordinates of all points and elements of the external orientation of the images have been computed by the bundle block adjustment. Exterior and interior parts of the church have been processed separately. Both parts were combined into one project using control points measured by a total station. The reconstructed three-dimensional model of the building comprises 4800 spatial points and 1600 surfaces determined from 46 digital images.

Because it was impossible to use the photogrammetric methods in the interior of the tower due to its narrow and elongated shape, a different approach had to be selected. A Trimble VX total station with built-in camera was used to measure the interior of the tower from the ground. This surveying instrument allowed us to scan the surface at a velocity of up to 10 points per second and under zenith angles of incidence close to zero. The entire vector model displayed in Figure 4 includes all surfaces of interior and exterior parts of the church and the tower. The mean squared error of unit weight after the bundle adjustment is 1.12 pixels, which represents an achieved accuracy of 0.003 mm in the image plane. A total model accuracy of 0.018 m (a spatial mean error) calculated from all points was achieved.

Geophysical methods

Non-destructive geophysical methods have been applied successfully in many surveys to detect and investigate features of archaeological interest (e.g. Clark, 1990; Schmidt, 2001; Gaffney and Gater, 2003). Nowadays, integrated geophysical surveys play an important role in the non-invasive exploration of archaeological sites. Ground-penetrating radar is a fast electromagnetic technique based on high-frequency electromagnetic wave propagation that is designed primarily to investigate the shallow subsurface of the Earth. The literature records many case studies where the GPR method was successfully applied in sacral building exploration (e.g. Conyers, 2004; Leucci, 2006;

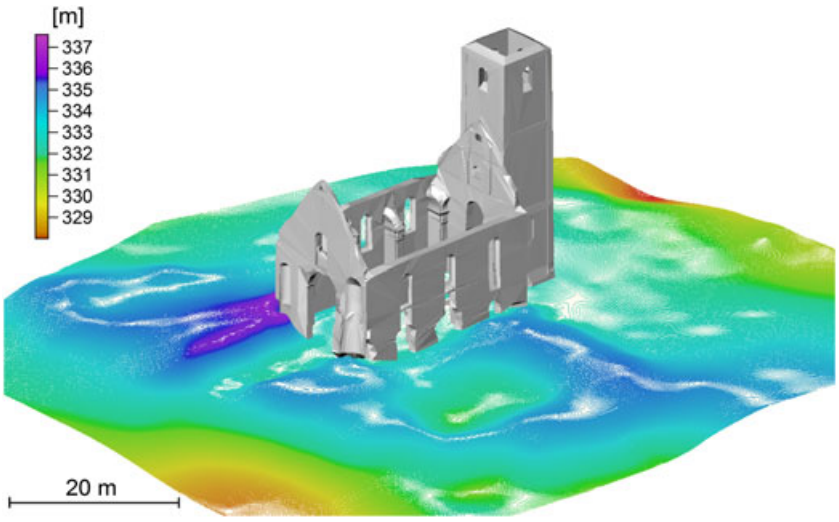

Figure 4. The polyhedral model of the church displayed along with the surrounding topography. This figure is available in colour online at wileyonlinelibrary.com/journal/arp

DOI: 10.1002/arp

Blanco *et al*., 2008; Udphuay *et al*., 2010; Cataldo *et al*., 2012). Microgravity is a geophysical method based on highly accurate measurement and interpretation of very small variations in the Earth's gravitational field, by which the subsurface archaeological features of contrasting or anomalous density can be detected. In spite of the time-consuming data acquisition, processing and inherent ambiguity of source determination, the microgravity technique has been used for cavity detection at many archaeological sites during the past decades (Blížkovský, 1979; Lakshmanan and Montlucon, 1987; Cuss and Styles, 1999; Abad *et al*., 2007; Pašteka *et al*., 2007; Panisova and Pašteka, 2009; Padín *et al*., 2012).

Microgravity

The microgravity survey was undertaken to investigate the area inside the former church. This area was surveyed on a closely spaced grid of 258 stations (Figure 5) with a point spacing of 1 m. A Scintrex CG-5 gravimeter was used to acquire the gravity data. The readings were corrected automatically for Earth's tide variations. The instrumental drift was estimated by regularly repeated readings at a selected base station at hourly intervals and semi-random returns to other stations within the grid. The daily drifts of the CG-5 gravimeter varied in the range of 21 to 57 μGal during five measuring days with an almost linear character of the individual drift curves. Statistical analysis of the repeated station values from different days (i.e. 11% from the total number of points) provided a mean squared error of less than 4 μGal in the measured gravity. The height of each survey point was obtained using a simple level with a closed-loop accuracy of approximately 13 mm. The horizontal coordinates of the gravity stations were determined by a Trimble M3 total station with a precision of 30 mm.

The Bouguer anomalies were calculated as follows (Panisova *et al*., 2012):

$$\Delta g_B(P) = g(P) - [-0.3086\ h(P) + 0.0419\ \rho h(P^*) - T(P)] + K(P), \quad (1)$$

where $g(P)$ is the measured gravity value corrected for instrumental drift and the Earth's tides, the first two terms in the brackets are the free-air and planar Bouguer corrections, $T(P)$ is the terrain correction, $K(P)$ is the building correction, $h(P)$ and $h(P^*)$ are the elevations at gravimeter sensor position P and its vertical projection P^* to the surface and ρ is the correction density. Microgravity surveys are generally concerned with the relative variations in the local gravity field, thus conversion of readings to absolute gravity was unnecessary (Cuss and Styles, 1999). The latitude correction was not considered because of the small dimensions of the surveyed area. A density of 2.4 g cm $^{-3}$ was used for the calculation of the planar Bouguer and

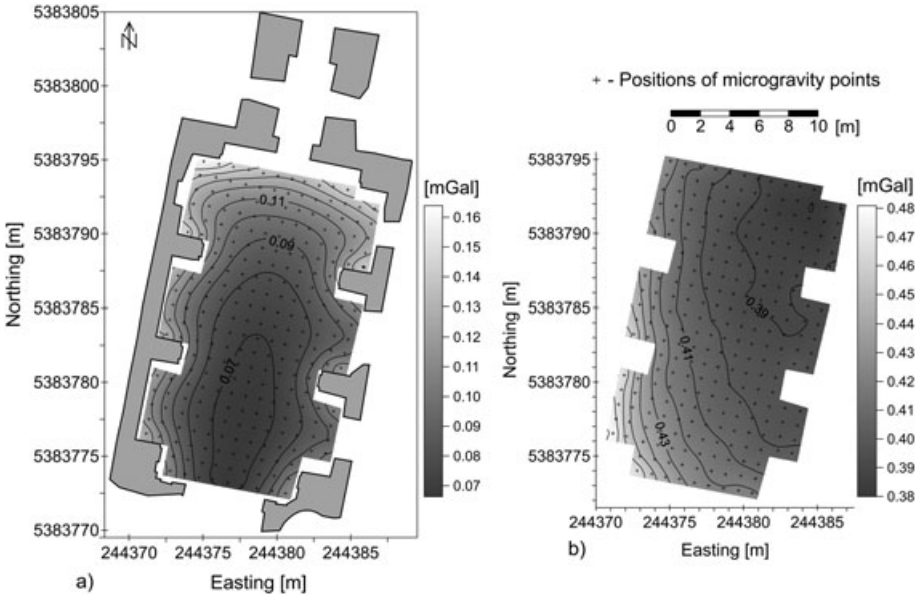

Figure 5. (a) The building correction in mGal computed from the polyhedral model for an estimated density of 2.2 g cm $^{-3}$ displayed within the plan of the church. (b) The terrain corrections in mGal calculated up to a distance of 5.24 km.

DOI: 10.1002/arp

terrain corrections. The site is characterized by a complex geology and rather rugged surrounding topography. The land around the gravity stations was therefore mapped using a Trimble M3 total station and a detailed topographic model (Figure 4) within a 30 m zone surrounding the microgravity grid was constructed. Consequently, it was used for the calculation of the innermost zone terrain correction. The inner zone terrain correction was computed up to a distance of 250 m using a digital elevation model (DEM) with a 10 m grid spacing. The threshold distance (outer radius) of 5.24 km, where the far zone terrain contributes more or less equally to all microgravity points, was determined and the corresponding far zone terrain correction was calculated using a DEM with 50 m grid spacing. The cumulative terrain corrections are displayed in Figure 5b.

Building correction is very important in microgravity surveys when large structures are present. This correction allows to correct for the gravitational attraction arising from the mass of the existing man-made structures as their effects can be greater than the amplitude of the expected anomalies (Debeglia and Dupont, 2002). The final model of the church (Figure 4) obtained from photogrammetric processing served as the direct input to our program (Panisova *et al.*, 2012), which is based on the three-dimensional polyhedral body approximation introduced by Götze and Lahmeyer (1988). The model of the church was exported from PhotoModeler 6 in 'raw' format as one polyhedral body defined by 4306 points and 8148 triangles. In our program the attraction effect of this body was calculated as the summation of the integrations along the line elements of its individual faces using the equation of Götze and Lahmeyer (1988). The walls of the church comprise limestone and travertine stones, bricks, oak beams and lime mortar (Herceg, 2009). The building correction (Figure 5a) was calculated for a mean density of 2.2 g cm^{-3} estimated from catalogues of densities for building materials. The maximum amplitude of the building correction reaches 160 μGal in the northern part of the map shown in Figure 5a due to the presence of the church tower with relatively great wall thickness – 2 m. The processed data were contoured to yield a Bouguer anomaly map (Figure 6).

In the Bouguer anomaly map shown in Figure 6, only the distinctive negative anomaly produced by the excavated crypt is clearly identifiable (in the upper northeast corner of the grid). This negative anomaly is superimposed upon a complex long-wavelength regional feature, which slopes from west to east and is with high probability caused by the dipping bedrock

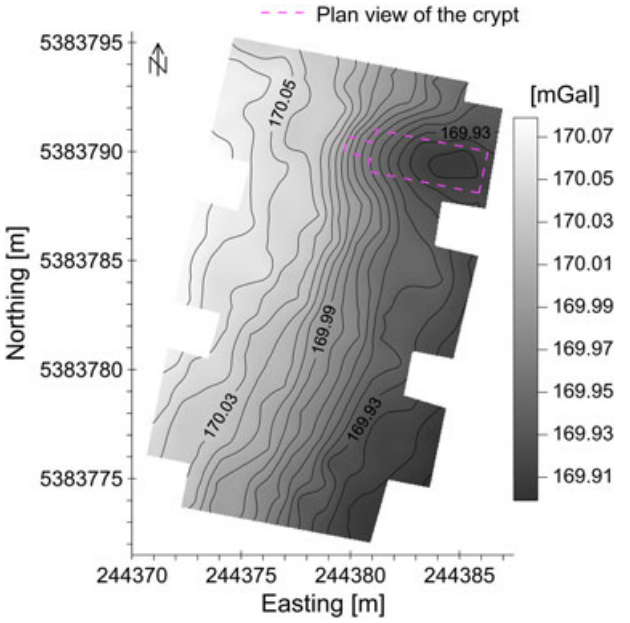

Figure 6. Bouguer anomalies in mGal calculated for a correction density of 2.4 g cm^{-3}. This figure is available in colour online at wileyonlinelibrary.com/journal/arp

of Middle Triassic carbonates. For the regional residual-field separation, a first-order polynomial (planar surface) was fitted to the data in Surfer software (www.goldensoftware.com). The removal of this strong regional trend revealed several previously unrecognized anomalies in the resulting residual Bouguer anomaly (Figure 7a). Over the surveyed area, residual anomalous gravity values fell within the range −47 to +33 μGal. Two interpretation methods, namely Euler deconvolution and harmonic inversion, were used for the estimation of the depth and size of the anomalous sources.

Euler deconvolution is an interpretation technique for locating the sources of potential fields based on both their amplitudes and gradients and an estimate of the probable geometry of the causative body (Reid *et al.*, 1990). This technique is very appropriate for use in microgravity surveys, where high quality and closely spaced data are available (Cuss and Styles, 1999). Software developed at the Comenius University in Slovakia was used to solve for the depth estimate to anomalous sources. A window of specific size is moved across the gridded data, using least-squares inversion to solve Euler's homogeneity equation with regularized derivatives incorporated (Pašteka *et al.*, 2009). The structural index related to the attenuation with distance of the potential field was set to one (detecting a horizontal cylinder in gravimetry). The selected Euler solutions in the area of the calculated density model are shown by filled black circles in Figure 7.

DOI: 10.1002/arp

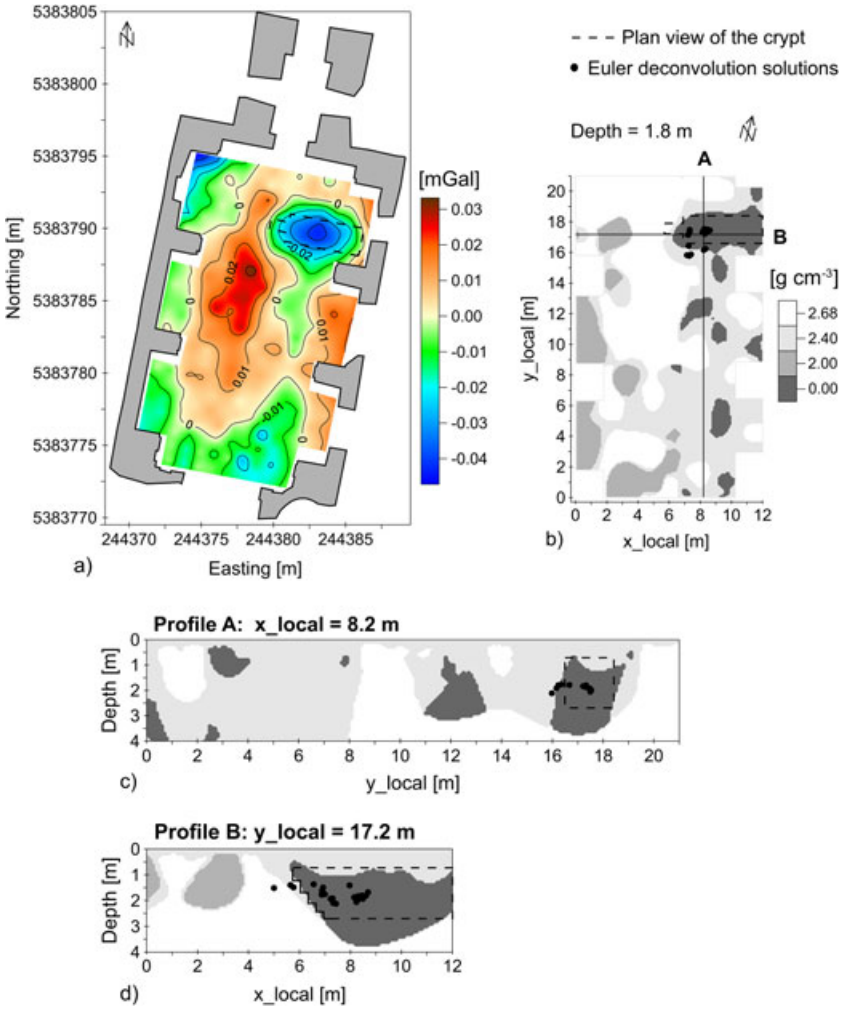

Figure 7. (a) Residual Bouguer anomaly map in mGal obtained by planar trend subtraction from the Bouguer anomaly map in Figure 6. (b) The interpretation of the microgravity results using the harmonic inversion and Euler deconvolution methods for a depth of 1.8 m. (c and d) The density distributions in two vertical sections for profiles A and B; the filled circles denote the positions of the three-dimensional Euler deconvolution depth estimates. This figure is available in colour online at wileyonlinelibrary.com/journal/arp

The harmonic inversion method for three-dimensional gravity data inversion was presented and described in detail in Pohánka (2003a, 2003b). This method solves the inverse gravimetric problem in two steps. First, the measured surface gravitational field, namely the residual anomalies obtained by the regional trend removal from the Bouguer anomalies (Equation 1), is transformed into so-called quasigravitation. The quasigravitation is a function satisfying the following conditions: (i) it is a sufficiently smooth (triharmonic) function; (ii) it is a linear integral transformation of the surface gravitational field; and (iii) for the gravitational effect of point sources it has its main extremum at the point source (Pohánka, 2003b). Then using the calculated quasigravitation the position and shape of a set of anomalous bodies embedded in an a priori known horizontally layered background, so called multidomain density model, is found iteratively. Specifically, the germs of future anomalous bodies defined as elementary cubes are placed at the local extrema of the calculated quasigravitation in the starting model. The densities of every single body are the only free parameters that have to be assigned. Consequently, the shape of bodies is modified from the original germs by adding or removing additional elementary cubes at body boundaries only. In each iterative step the gravitational effect of the current shape of the bodies is calculated, and the residual surface field is obtained by subtraction from the original one. Then the residual quasigravitation is recalculated and the process is repeated until the residual surface field becomes satisfactory small. This approach for the calculation of a density model greatly accelerates and simplifies the finding of a solution,

DOI: 10.1002/arp

because the three-dimensional density distribution is calculated from the three-dimensional quasigravitation function instead of the two-dimensional gravitational field.

The residual Bouguer gravity anomaly field displayed in Figure 7a served as the input to the calculation of the density distribution. In our case the background consists of a single layer with a density of $2.4\,g\,cm^{-3}$ defined from the surface to 4 m depth. In the starting model the densities of possible anomalous bodies were chosen as $0.0\,g\,cm^{-3}$ (empty cavities), $2.0\,g\,cm^{-3}$ (partially filled cavities or lighter material) and $2.68\,g\,cm^{-3}$ (heavier bedrock outcrop). The final three-dimensional density distribution (depth-slice and vertical sections displayed in Figure 7) was calculated after 352 iterations.

Ground-penetrating radar (GPR)

The area of prospection included most of the inside area of the church, but only the data set from the GPR survey carried out in the eastern half of the nave is presented here, where beside the mentioned object another two aristocratic crypts are supposed to be located. A GSSI SIR-20 system was used with a 400 MHz antenna. Thirty-six GPR profiles were acquired in zigzag mode with 0.15 m line spacing. A map of the location of the profiles is shown in Figure 8a. For time/depth conversion, the electromagnetic wave propagation velocity was estimated by diffraction hyperbola fitting with an average value of $0.09\,m\,ns^{-1}$ in the subsurface of the surveyed area (Figure 8b). The good quality of the raw data did not require advanced processing techniques. Processing steps for each profile consisted of t_0 corrections, offset removal and direction ordering. To correct for t_0 several methods are presented in the literature (e.g. Yelf and Yelf, 2006). In this study we used the mean first break position as t_0 and shifted the whole radargram backwards in time. The offset removal was done by calculating a mean trace for each radargram and subtracting it from all traces. This

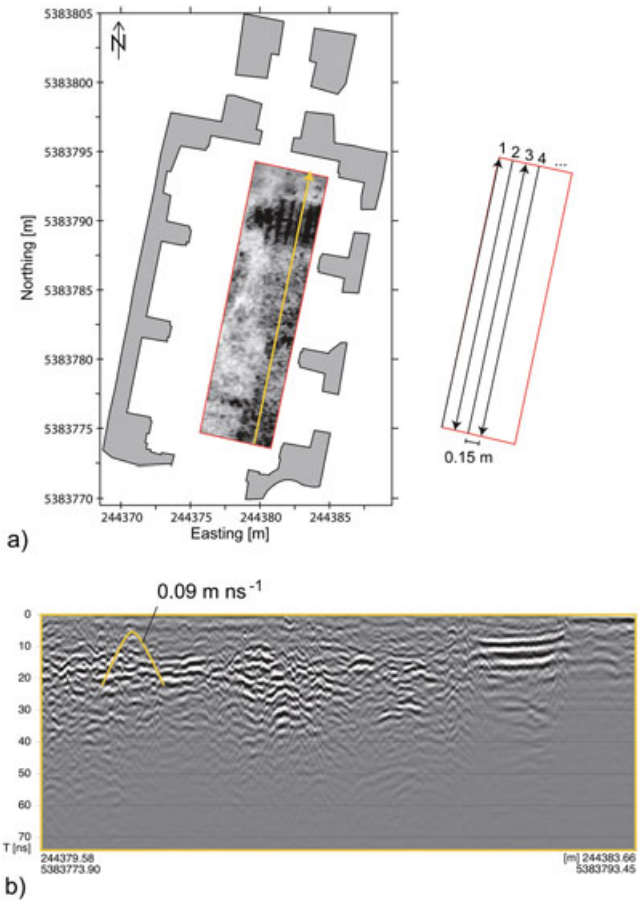

Figure 8. (a) Location of the area that was measured with GPR in zigzag mode and location of the exemplary profile in (b). The horizontal time-slice shown is a stack between 0 and 20 ns (approximately 0–0.9 m depth). (b) Exemplary profile for the velocity determination by fitting of a diffraction hyperbola. This figure is available in colour online at wileyonlinelibrary.com/journal/arp

DOI: 10.1002/arp

processing step eliminates horizontal events such as the ground and air wave and thus highlights non-horizontal structures. Due to the acquisition in zigzag mode the last processing step was to flip every second radargram so that they are all run from south to north for better visualization.

Then horizontal time-slices were created by interpolation between the profiles and summing the absolute reflection amplitudes in certain time windows. To enhance the most significant subsurface features being visible in several time-slices, we stacked the corresponding time-slices. The time to depth conversion can be done by dividing the two-way-travel time by two and multiplying it with the velocity of $0.09\,\mathrm{m\,ns^{-1}}$.

The results from the GPR survey were visualized for the qualitative interpretation in the form of horizontal time-slices and vertical time-sections (Figure 9). The GPR horizontal time-slices shown in Figure 9 are the visualizations of the most significant subsurface features within 0–20 ns (approximately 0–0.9 m depth, Figure 9a) and within 20–40 ns (approx. 0.9–1.8 m depth, Figure 9b). The GPR time-sections presented in Figure 9c and d (Profiles A and B in Figure 9b) correspond to about 0–3.2 m in depth.

In the shallow time-slice, high-amplitude reflections related to the known air-filled crypt are dominant (Figure 9a – northern part of the surveyed area). In the deeper time-slice, two distinctive reflection anomalies indicate the existence of two other features of archaeological interest (Figure 9b – central and southern part of the surveyed area). These two new features, which do not seem to be interconnected, are interpreted as two aristocratic crypts documented in the archives of the Roman Catholic Manse in Dechtice.

In the vertical time-section (Figure 9c) the top of the known air-filled crypt (C1) is indicated by a strong almost horizontal reflection, which is caused by the dielectric permittivity contrast between soil or concrete and air. The hyperbolic reflection below is caused by a post, which was installed to support the concrete cover (Herceg, 2009, Peter Herceg, personal communication, 2012). The second almost horizontal reflection at about 25 ns can be interpreted as the bottom of the crypt, taking the high velocity in air ($0.30\,\mathrm{m\,ns^{-1}}$) into account.

The chaotic reflection patterns of features C2 and C3 lead us to suggest that the expected crypts are destroyed and filled by debris. No clear reflections of top or bottom of the expected crypts are visible. Nevertheless, the depth to the top of these crypts is estimated to be around 0.5 m. These chaotic reflections also can be found on several parallel profiles on the eastern edge of the measured area, which is indicated in the time-slices by areas of high reflection energy (dark). Another area of higher reflection energy at the western edge of the time slices is associated with slightly northwards dipping reflections at about 1 m depth (Figure 9d), the origin or meaning of which is not clear, but might be associated with the bedrock. The interpretation of the westward oriented appendages on two deeper anomalies in Figure 9b is not clear. The chaotic reflection patterns might indicate debris or incised staircases, as shown in Figure 2 for the known crypt.

Discussion

The harmonic inversion method provides several admissible subsurface density models for the recorded residual gravity field, so comparison with other interpretation techniques as well as other geophysical methods is necessary to select the most feasible one. For determining the shape of anomalous bodies more accurately, an increase in the density of microgravity points is required. In Figure 7b, the density distribution for 1.8 m depth obtained by means of harmonic inversion is displayed, along with the Euler deconvolution solutions denoted by filled circles. Figure 7c and d shows selected vertical sections of the density model in two profiles crossing the main gravity low produced by the known crypt. The average depth (approximately 1.6–2.0 m) of the solution cluster, located around 8 m in the x direction and 17 m in the y direction, fit into the estimated depths of the air-filled crypt obtained by means of the harmonic inversion method. In the case of the other predicted crypts, no solution cluster by means of the Euler deconvolution method was obtained. This is probably due to the low amplitude and weakly developed gradients of these anomalies. The vertical density section (Figure 7c) can be correlated with features seen on the GPR vertical time-section (Figure 9c). The low-density area between 16 and 18 m (Figure 7c, known air-filled crypt) corresponds to feature C1 in the GPR vertical time-section (Figure 9c) and approximately at the locations of features C2 and C3 two other low-density areas can be found.

This case study illustrates the advantage of combining geophysical methods that are based on different physical parameters. In order to eliminate the ambiguity inherent in each method, the residual Bouguer anomaly map and GPR horizontal time-slices were overlapped and compared (Figure 9a and b). For the air-filled crypt excavated in 2001, the dimensions ($5 \times 1.9 \times 2$ m) and position (its top

DOI: 10.1002/arp

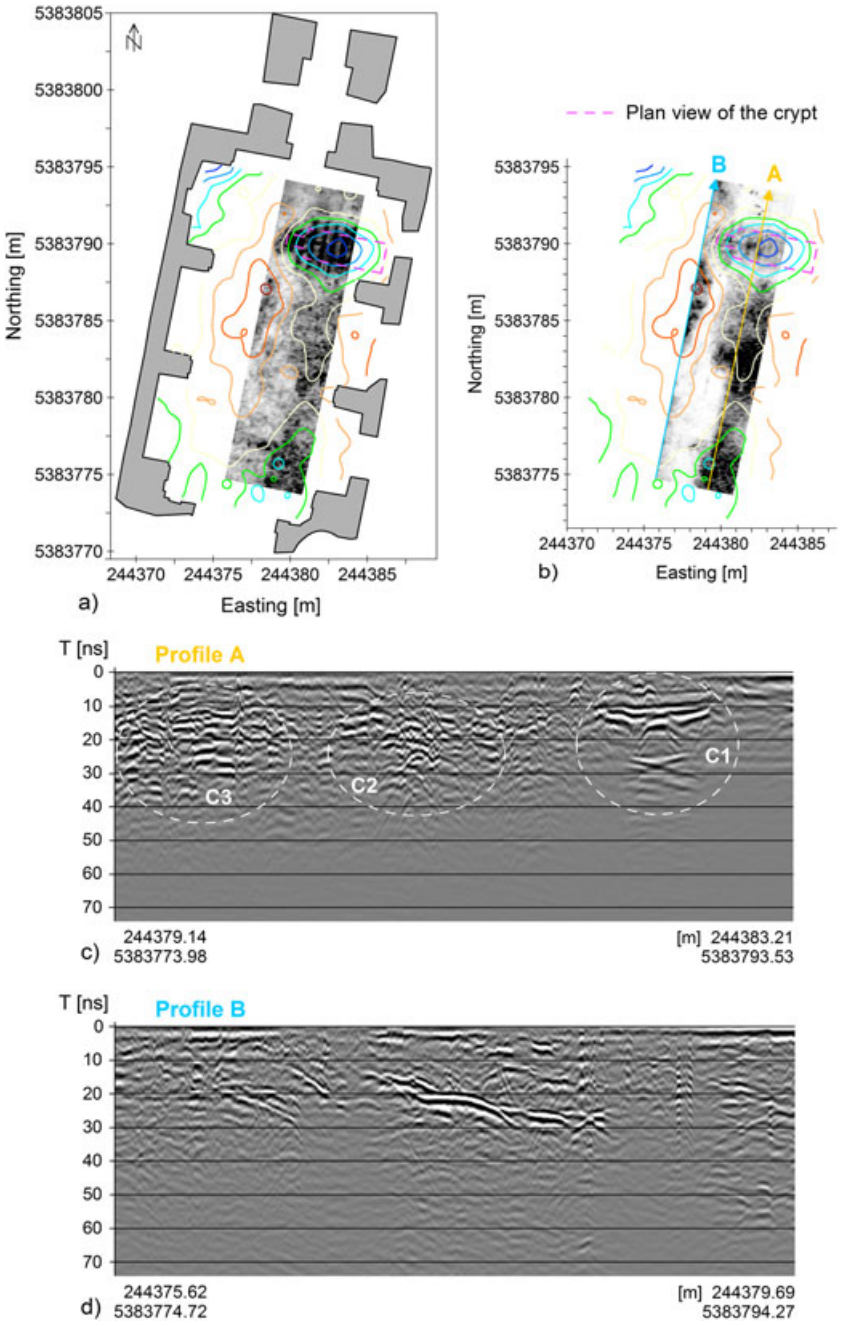

Figure 9. The GPR results. (a) Horizontal time-slice stack between 0 and 20 ns (approximately 0–0.9 m depth) displayed along with the residual Bouguer anomaly contours. (b) Horizontal time-slice stack between 20 and 40 ns (approximately 0.9–1.8 m depth) displayed along with the residual Bouguer anomaly contours. (c) Vertical time-section (Profile A) running in SW–NE direction. (d) Vertical time-section (Profile B) running in SW–NE direction. This figure is available in colour online at wileyonlinelibrary.com/journal/arp

is situated at a depth of 0.6–0.8 m below the ground) have been confirmed by both geophysical methods. The slightly larger outline of the crypt in the GPR time-slices is explained by indications of diffraction hyperbolas from the corners of the crypt. The other two features, which were successfully detected and delineated by both methods, are with high probability the predicted crypts. The GPR and microgravity results indicate that these two features could be partially filled. Recommendations for archaeological excavation were given to the site-excavators.

DOI: 10.1002/arp

Conclusions

An integrated geophysical approach to detect and characterize subsurface archaeological features has been applied in the nave of the former St Catherine's church. The combination of GPR and microgravity techniques is shown to be a very effective and non-destructive tool for such mapping. In the GPR survey carried out on the eastern part of the nave several reflection anomalies, caused by buried structures interpreted as crypts, have been found. In the microgravity survey a novel approach of microgravity data processing has been employed. A detailed three-dimensional polyhedral model used in the calculation of the building correction was reconstructed from photographs of the church with a special photogrammetric software. The microgravity technique has confirmed the position and size of the known aristocratic crypt excavated in 2001. Moreover, in correlation with GPR it suggests the presence of other structures that are most likely to be related to two crypts documented in historical archives. The geophysical results obtained could be incorporated to the virtual databases, where valuable monuments are documented for next generations.

Acknowledgements

This work was performed mainly with the support of the VEGA Slovak Grant Agency under projects No. 1/0680/10, 1/0095/12 and 2/0067/12, partially with the support of the Slovak Research and Development Agency under the contracts No. APVV-0194-10 and APVV-0724-11. We would like to thank Peter Herceg, Ivana Kvetánová and Jozef Urminský for essential information regarding the archaeological survey of the site. We would like to express our gratitude to Professor Hans-Jürgen Götze and Dr Sabine Schmidt from Kiel University for the subroutine that calculates the gravity effect of triangle. We are also grateful to Vladimír Pohánka from the Geophysical Institute of the Slovak Academy of Sciences for his scientific support with the calculation of the subsurface density distribution using his harmonic inversion method. We would also like to thank the participants of the INCA course (International Course on ArchaeoGeophysics) 2009 for the measurement of the GPR data.

References

Abad IR, García FG, Abad IR, *et al*. 2007. Non-destructive assessment of a buried rainwater cistern at the Carthusian Monastery 'Vall de Crist' (Spain, 14th century) derived by microgravimetric 2D modelling, Case study. *Journal of Cultural Heritage* **8**(2): 197–201.

Blanco MR, García FG, Abad IR, Sala RM, Benlloch J. 2008. Ground-penetrating radar survey for subfloor mapping and analysis of structural damage in the Sagrado Corazón de Jesús Church, Spain. *Archaeological Prospection* **15**(4): 285–292. DOI: 10.1002/arp.341.

Blížkovský M 1979. Processing and applications in microgravity surveys. *Geophysical Prospecting* **27**(4): 848–861.

Bodoriková S, Katina S, Kováčová V, *et al*. 2010. Analysis of trace elements in the teeth of individuals from the former crypt in St. Catherine's monastery in Dechtice (District Trnava, Slovakia). *Scripta Medica* **83**(1): 49–58.

Cataldo R, D'Agostino D, Leucci G. 2012. Insights into the buried archaeological remains at the Duomo of Lecce (Italy) using ground-penetrating radar surveys. *Archaeological Prospection* **19**(3): 157–165. DOI: 10.1002/arp.1423.

Clark A. 1990. *Seeing Beneath the Soil: Prospecting Methods in Archaeology*. Bathsford: London.

Conyers LB. 2004. *Ground-penetrating Radar for Archaeology*. AltaMira Press: Walnut Creek, CA.

Cuss RJ, Styles P. 1999. The application of microgravity in industrial archaeology: an example from the Williamson tunnel, Edge Hill, Liverpool. In *Geoarchaeology: Exploration, Environments, Resources*, Pollard AM (ed). Special Publication 165, Geological Society: London; 41–59.

Debeglia N, Dupont F. 2002. Some critical factors for engineering and environmental microgravity investigations. *Journal of Applied Geophysics* **50**(4): 435–454.

Fraštia M. 2005. Possibilities of using inexpensive digital cameras in applications of close-range photogrammetry. *Slovak Journal of Civil Engineering* **8**(2): 20–28.

Gaffney C, Gater J. 2003. *Revealing the Buried Past: Geophysics for Archaeologists*. Tempus Publishing: Stroud.

Götze HJ, Lahmeyer B. 1988. Application of three-dimensional interactive modeling in gravity and magnetic. *Geophysics* **53**(8): 1096–1108.

Herceg P. 2009. *Experiences with the restoration of St. Catherine's monastery ruins. 15 years of St. Catherine's monastery preservation project near Dechtice village*. Association of the Christian Youth Communities: Spišská Nová Ves. (In Slovak.)

Lakshmanan J, Montlucon J. 1987. Microgravity probes the Great Pyramid. *The Leading Edge* **6**(1): 10–17.

Leucci G. 2006. Contribution of ground penetrating radar and electrical resistivity tomography to identify the cavity and fractures under the main church in Botrugno (Lecce, Italy). *Journal of Archaeological Science* **33**(9): 1194–1204.

Luhmann T, Robson S, Kyle S, Harley I. 2006. *Close Range Photogrammetry: Principles, Techniques and Applications*. Whittles Publishing: Dunbeath.

Matulová M. 2003. *The St. Catherine monastry close to Dechtice*. MSc thesis, Comenius University Bratislava; 88 pp. (In Slovak.)

Padín J, Martín A, Anquela AB. 2012. Archaeological microgravimetric prospection inside don church (Valencia, Spain). *Journal of Archaeological Science* **39**(2): 547–554.

Panisova J, Pašteka R. 2009. The use of microgravity technique in archaeology: A case study from the St. Nicolas Church in Pukanec, Slovakia. *Contributions to Geophysics and Geodesy* **39**(3): 237–254.

Panisova J, Pašteka R, Papčo J, Fraštia M. 2012. The calculation of building corrections in microgravity surveys using close range photogrammetry. *Near Surface Geophysics* **10**(5): 391–399. DOI: 10.3997/1873-0604.2012034.

Pašteka R, Zahorec P. 2000. Interpretation of microgravimetrical anomalies in the region of the former church of St. Catherine, Dechtice. *Contributions to Geophysics and Geodesy* **30**(4): 373–387.

Pašteka R, Terray M, Hajach M, Pašiaková M. 2007. Microgravity measurements and GPR technique in the search for medieval crypts: a case study from the St. Nicholas church in Trnava, SW Slovakia. Proceedings of the Archaeological Prospection 7th Conference, Nitra. *Štúdijné zvesti* **41**: 222–224.

Pašteka R, Richter P, Karcol R, Brazda K, Hajach M. 2009. Regularized derivatives of potential fields and their role in semi-automated interpretation methods. *Geophysical Prospecting* **57**(4): 507–516. DOI: 10.1111/j.1365-2478.2008.00780.x.

Pohánka V 2003a. The harmonic inversion method: calculation of the multi-domain density. *Contributions to Geophysics and Geodesy* **33**(4): 247–266.

Pohánka V. 2003b. *Testing of two variants of the harmonic inversion method on the territory of the eastern part of Slovakia*. http://gpi.savba.sk/GPIweb/ogg/pohanka/East1.ppt (accessed 20 September, 2003).

Reid AB, Allsop JM, Granser H, Millett AJ, Somerton IW. 1990. Magnetic interpretation in three dimensions using Euler deconvolution. *Geophysics* **55**(1): 80–91.

Schmidt A. 2001. *Geophysical Data in Archaeology: A Guide to Good Practice*. Oxbow Books: Oxford.

Udphuay S, Paul VL, Everett ME, Warden RB. 2010. Ground-penetrating radar imaging of twelfth century Romanesque foundations beneath the thirteenth century Gothic abbey church of Valmagne, France. *Archaeological Prospection* **17**(4): 199–212. DOI: 10.1002/arp.383.

Urminský J. 2002. Continuation of the investigation of St. Catherine's monastery near the Dechtice village. *Archaeological Explorations and Finds in Slovakia in 2001*. Archaeological Institute of Slovak Academy of Sciences: Nitra; 215–216. (In Slovak.)

Yelf R, Yelf D. 2006. Where is true time zero? *Electromagnetic Phenomena* **7**(1–18): 158–163.